The Cryosphere Discuss., 8, C3200–C3214, 2015
www.the-cryosphere-discuss.net/8/C3200/2015/

The Cryosphere
Discussions
Open Access

Interactive comment on "Thermal energy in dry snow avalanches" *by* W. Steinkogler et al.

W. Steinkogler et al.

steinkogler@slf.ch

Received and published: 19 March 2015

We thank the reviewer for the very detailed comments. The insight and criticism helped us to produce a better and more accurate analysis, which will be presented in a revised paper version.

1 General comments 1.1 Summary of goals, approaches and conclusions Steinkogler et al. studied the thermal properties of three artificially released dry avalanches. The aim was to estimate potential sources of thermal energy in an avalanche. As a minor aim the authors wanted to investigate the application potential of an infrared camera for measuring the spatial temperature distribution of an avalanche. The temperature distribution of the avalanches was quantitatively measured with thermometers regularly used in snow pits, snow depth probes with attached thermistors, and rather qualitatively with an infrared camera. With snow profiles the authors could identify warmer snow

temperatures in the deposition of the avalanche than anywhere else in the undisturbed profiles next to the avalanche. The authors concluded with these observations that entrainment cannot explain these relatively warm snow temperatures in the deposition zone. After theoretically excluding other sources, friction was discussed to be the main reason for this observation. Furthermore, the authors concluded that warming due to friction was mainly dependent on the elevation drop, while warming due to entrainment was dependent on many factors related to the specific avalanche. Lateral temperature variations in the depositions of the avalanche were related to assumed flow regimes of the avalanche.

1.2 Evaluation of the overall quality

RC: Studying the temperature distribution in an avalanche is worthwhile and will provide relevant verification data to avalanche dynamic models. The identification of friction as a major thermal energy source in an avalanche is new to my knowledge. Also, the use of an infrared camera is new for this purpose, although the relevant results were obtained by traditional measurements. The purpose of the work is clear and appropriate methods were used to address the questions (except for the validation of the infrared camera, see comments below). The manuscript is written in a clear and concise manner and in good English. The figures are well prepared and add to the understanding of the manuscript. The relevance of this manuscript lies in the identification of friction as major thermal energy source. This impact can be enhanced with a better literature review of other measuring and modelling attempts of friction in dry snow avalanches.

AC: We now provide additional literature on the proposed measuring and modeling approaches. Special focus is put on the potentially large variations of thermal energy due to entrainment.

RC: Furthermore, I think it is within the scope of such a contribution to include an avalanche dynamic model with the purpose of (i) to initially verify the friction implemen-

tation (which was mentioned in the Conclusions as an outlook) and (ii) to better quantify the thermal energy contribution of friction considering mass entrainment and deposition along the path. This would shift the rather descriptive manner of this manuscript to a more analytical manner, and would more clearly answer the question how relevant friction is for avalanche dynamics.

AC: We agree with the reviewer on the fact that a more detailed conceptual treatment of the thermal energy contributions is needed. We therefore now present a mass dependent calculation which addresses the reviewer request to improve the descriptive manner of this part of the paper. This includes a representation of the bulk effect of entrained snow, which may be at a different temperature compared to the released snow. We do not aim to include a more complex numerical avalanche dynamics model in our paper as we aim to provide initial experimental data that can be used to further verify and improve such models. The additional analysis that will be presented in the revised version maintains that frictional heating is correctly described by the equation originally presented. We made an effort, however, to point out that the equation in general describes the loss of potential energy as a mass increment or finite volume descends a slope. Taking this into consideration, the drop height had to be adapted in the refined calculations, confirming however that frictional heating is the dominant term. The refined calculations now show explicitly the contribution of entrained snow to frictional heating. The contribution that entrained snow has because of its different temperature is small for our cases but is also explicitly calculated in the revised version.

In the following I will focus on the questions, if the results support the conclusions, if the aim to investigate the usability of an infrared camera is met, and if the methods used are appropriately described. I am convinced the authors are able to address my specific comments below. Thus I recommend to publish this manuscript in The Cryosphere after Major Revisions.

2 Specific comments 2.1 Do the results support the conclusions? RC: I understand what it means to gather data from real avalanche experiments, which prevents to in-

clude several boundary conditions. But the main conclusions of the manuscript are formulated in a too general way, which is not supported by the data collected from two (three) studied avalanches under quite similar conditions. Other important conclusions are rather supported my common knowledge than by own data. I suggest a more careful wording of the following conclusions: 2.1.1 Friction is mainly dependent on the elevation drop “Our results confirm that for the investigated avalanches the thermal energy increase due to friction is mainly depending on the elevation drop of the avalanche and thus a rather constant value (for a specific avalanche path and typology)” (in the Abstract). The authors could not investigate avalanches with several different elevation drops to justify this statement. Only an oversimplified friction calculation supports the statement that friction is mainly dependent on elevation drop. This generalization is especially problematic since the authors were not able to separate the sources of warming. I suggest a less generalizing formulation.

AC: We agree with the reviewer that the main conclusions were formulated too general. We therefore now provide a more detailed analysis of the friction and entrainment contribution to the overall warming (see our detailed response to comment 1.2 of Reviewer 1 above). As suggested we will reformulate the conclusions to clearer distinguish results that can be transferred to other situations and results that are only valid for the specific avalanches investigated in this study.

2.1.2 Entrainment is very specific RC: “... warming due to entrainment was very specific to the individual avalanche and depended on the temperature of the snow along the path and the erosion depth ...” (in the abstract). Similarly, the authors could not investigate avalanches with different entrainment characteristics and their impact on warming. AC: We will change this formulation in the abstract. In the paper we now describe the mass balance in more detail. Furthermore, we now clearly separate the contributions due to friction and entrainment. We now can show that indeed there is a difference in the entrainment characteristics of the investigated avalanches. However the reviewer is correct in observing that the entrainment is not so “important” for the

thermal balance in these two cases. In fact, while the entrainment characteristics of the two avalanches are quite different (avalanche 2 is characterized by a growth index Ig=me/mr=of 3.7 while avalanche 3 as Ig=1.6) the temperature difference between release and entrained snow is almost negligible for avalanche #2. This makes friction the main contribution for the warming of the deposit, in this specific case. This is now better described in the paper.

RC: The conclusion is based on general knowledge of a temperature gradient in the snowpack (p. 5806, line 5ff) and the observation of different surface temperatures on the bed surface of two avalanches.

AC: The reviewer is correct that this conclusion cannot be based on the specific measurements we have analyzed since in our case entrainment has a small contribution in the overall thermal balance. We will reformulate this specific conclusion but discuss what we may expect if the entrainment goes into deeper and warmer layers. Yet, we are not sure whether the reviewer misunderstood our method to calculate the temperature of the entrained snow. Since the thermal balance for the two avalanches is based on measurements, combining TLS data and manual snow profiles to assess the depth of the entrained layer and the respective temperatures, our results are based on measurements and not on general knowledge of a temperature gradient in the snow cover.

RC: The authors should consider rewording which indicates that this statement is rather based on reasonable theoretical considerations and common knowledge (temperature gradient in snowpack and irregular entrainment and erosion depth) than from own collected data.

AC: We reworded our statements to be clear where we refer to our measurements and where to literature.

2.1.3 Relation between flow regime and thermal signal RC: Throughout the manuscript the authors relate the thermal signal with different flow regimes, e.g. in Figure 7 and in

the text: “Lateral profiles ... allowed to differentiate between undisturbed snow cover, the deposits of a fluidized layer ... and the dense core.” (p. 5802 line 22ff). The authors observed differences of surface temperatures obtained by an infrared camera (Fig 7). The authors could hypothesize that these observed differences coincides with observations typical for different flow regimes. I do not think that the presented results are indeed allowing to identify deposits of different flow regimes. The authors did not describe in the methods that they systematically observed deposits indicating different flow regimes (Issler et al., 2008). This was much later added in the Discussion section. I suggest a more careful wording when relating thermal observations with assumed flow regimes. In the current way of writing I am not convinced that the authors knew exactly where the depositions of different flow regimes were located. Moreover, I doubt that the authors can be completely sure that mentioned flow regimes were existent in the studied avalanches. Cited authors only “believe” that a fluidized flow exists in dry snow avalanches (Gauer et al., 2008). I think the authors need to be clearer that they have a strong indication for this fluidized flow for their studied avalanches and know where the depositions were located (and communicate this accordingly), before they can be sure that the thermal signal allows to detect related deposits. This issue can also be solved with a more careful wording and a clearer communication of how the avalanche depositions were observed in the methods section.

AC: We added a description of the criteria for the identification of Issler et al., 2008 in the Methods section. In agreement with the reviewer comment we cannot be 100% sure that the observed lateral changes in the IRT measurements can be related to a fluidized layer (the same restriction applies to Issler et al., 2008 since direct in-flow measurements are lacking there as well). Yet, we think the IRT measurements are in agreement with observations in the deposits and the criteria formulated by Issler et al., 2008. They are therefore an informative addition to the other field observations. Regardless of whether the IRT signal differences arise from actual temperature differences or varying roughness, it appears that different areas in the deposits of an avalanche can be distinguished.

The reviewer is correct that the association of these regions to specific flow regimes is questionable, as questionable as the existence of a fluidized layer in avalanches is in the first place! As a compromise, in agreement with our own field observations we will replace “fluidized layer” with “thin deposit area” in a revised paper version. We will discuss in the discussion section possible reasons for these differences. It is clear that to finally answer this question, further field and laboratory studies will be necessary (see answer to comment 2.2 of reviewer 1).

The authors are convinced that the identified boundaries in the IRT data, the TLS and the measurements in the field match. This could be verified with GPS measurements, geo-referencing and matching persons visible in the IRT data with their GPS position. This also allowed us to locate the transects in Figure 6 and 7 as well as the locations of the point measurements in Figure 4. As suggested by the reviewer this will communicated more clearly in the revised paper.

2.2 Investigate the potential of the infrared camera RC: As a minor aim the authors wanted to investigate the application potential of an infrared camera for measuring the spatial temperature distribution (Introduction p. 5795 line 18ff; Conclusion p. 5810 line 1f). The authors only presented three data points, which is – as the authors stated – very basic. The authors used the camera in Figure 7 for a quantitative assessment of the surface temperatures. Additionally, they assigned different flow regimes to slight differences in this temperature, much less than 1 deg between an assumed fluidized layer and a dense core (Figure 7b). The cited literature (Schirmer and Jamieson, 2014) suggested that snow temperatures of a snow pit adapt fast and irregularly on a pit wall based on roughness after being exposed to the atmosphere. This case might be comparable: Avalanche deposits are similarly not in equilibrium with the atmosphere (as recognized by the authors, page 5809 line 6ff), and the deposits of assumed flow regimes may have a different surface roughness. This indicates that the situation described in the literature of a fast adaption of snow temperatures due to roughness differences may apply here as well.

AC: In contrast to Schirmer and Jamieson (2014), we did not investigate single roughness elements of convex or concave shape on the centimeter scale. With the used IRT cameras and objectives the pixel size of the footprint is approximately 1 m with the old camera model and 0.5 m with the new model (this information is now added to the methods sections). In our case we therefore receive an IRT signal which represents an average over the footprint area and has a more isotropic signal character than from a single roughness element. As shown in Figure 4, initially no large difference in cooling rates between relatively smooth bed surface of the release (IRT_release) and the rough debris areas (IRT_depo) could be measured. We agree with the reviewer that the effect of different roughness surfaces needs to be investigated further, preferentially with controlled laboratory experiments. We do not think that our data allows for more detailed conclusions due to limitations in control of atmospheric conditions, viewing angle, footprint size and distance between sensor and object (as discussed in the method section). Even if we cannot exclude possible absolute temperature errors due to superficial roughness, the different deposition areas can be clearly distinguished by the IRT camera. Since we only interpret these relative values in a qualitative way our conclusions are not affected by imprecisions in absolute temperatures.

RC: For the drawn conclusions (2.1.2 and 2.1.3) and for the proposed aim of investigating the potential of an infrared camera a more thorough validation is needed. My experience with measuring surface temperatures with metal thermometers is that they can be wrong by several degrees due to heating of diffuse solar radiation after shading the sensor. This means that the reference temperature used to validate the thermal camera is questionable. The comparison with a snow layer in a fracture line profile seems more promising.

AC: We agree with the reviewer that the measurements in the fracture line profile might be more reliable. The comparison measurements with the digital metal thermometers were conducted according to current snow profile standards. To answer this in more detail, laboratory experiments, similar to Schirmer and Jamieson (2014), should be

conducted.

RC: However, a potentially fast cooling of the fracture line was not investigated with the infrared camera.

AC: In all cases the (vertical) fracture line itself was too far away to allow for detailed investigations of its cooling. Yet, we investigated the surface temperature at the release area and but not the fracture line.

RC: Also, the authors have not stated how many minutes or seconds passed between the avalanche release and the infrared image used for this validation. The authors have taken videos of the release which provides data to address this known issue in more detail.

AC: The first images were acquired right after the release. For avalanche #1 and #2 only the older camera model was available which did not allow to record raw data with high, e.g. video, frame rates. Therefore the acquired videos are compressed files and do not allow to access the raw data directly. The new camera model, e.g. used for avalanche #3, would allow to record raw data at high frame rates and enable such analysis in future investigations.

RC: I suggest more careful wording when data of the IR camera is used and the potential is discussed. I would prefer if the authors add a more thorough validation of the infrared camera after an avalanche release, which can partly be done with existing data (how fast is the cooling, is the cooling speed different over different surface roughness, between the three avalanches representing different atmospheric conditions) or with new data.

AC: Figure 4 illustrates the available verification data. We now discuss this in more detail. A more elaborate verification requires laboratory setup and was out of scope for this paper.

2.3 Description of the methods 2.3.1 Infrared camera RC: Please provide necessary

information what the chosen emissivity value was, how the apparent temperature was determined, how the relative humidity was determined, how large the distance was from the camera to the avalanche (specifically to the transects in Figure 7), how large distance differences were from the constant value chosen for the whole image. I assume these values can be changed a posteriori and thus the sensibility of these values can be tested. Some minor changes may have large impacts on results caused by the rather large distances in this application. Please mention for Figure 7 how the pixel size was converted in meters.

AC: During all our experiments cold and dry snow conditions prevailed. We therefore chose an emissivity coefficient of 1 for the processing of our data. Again we want to point out here that our main aim was not to achieve highly accurate absolute temperature values and we did not go beyond an accuracy level as demonstrated in Figure 4. We also did not assign different emissivity values to different areas in the avalanche, which would technically be possible in post processing. Due to the dry snow conditions and the cold temperatures with low relative humidity a basic sensitivity study did not show drastic effects on the results, which have to remain mostly qualitative at present. In general, a validation of the IRT camera was out of scope of this paper. In this first approach the camera is used in a qualitative way to assess the spatial differences in temperatures. A nearby automatic weather station allowed to measure the relevant atmospheric parameters during the experiments. Information on the distance between the IRT camera and the release area below the rocks, which was around 800 m, will be added (also see comment 2.2. of reviewer 1 on pixel size of the footprint of the measurements). As the reviewer states, these values can be changed if raw data was recorded. Unfortunately this is not possible for the videos acquired during the release since this data is compressed. For the raw images that where acquired at regular intervals after the avalanche release a post-processing is possible.

RC: Much later was mentioned (for the determination of transported mass) that the image was georeferenced with a digital elevation model (DEM). Was the same method

applied for Figure 7?

AC: Information on geo-referencing and pixel to width conversion has already been provided in the response to comment 2.1.3. above.

RC: In the abstract it was mentioned that “this data set” was used to calculate the thermal balance, just after mentioning the infrared camera. This is confusing since only snow profiles were used for this purpose. For the mass assessment I assume these calculations are dependent on the quality of the DEM used for geo-referencing. Please provide the resolution, source and if available, error of the used DEM.

AC: We add this information to the revised paper.

2.3.2 Temperature probes RC: Please provide information of the vertical and horizontal resolution of the probing for Figure 8. For snow temperature measurements in snow profiles, the thermometers are regularly placed for a couple minutes to allow the sensor to adapt to the temperatures. Please provide the Time Constant for this sensor (and own experience when used in snow), your measuring time at one location, and the time used for one transect. Please also mention how the depth of the debris was determined (Fig. 8).

AC: For avalanche #2 a lateral trench was dug through the deposits which allowed to perform regular digital thermometer measurements, as well to measure the depth of the deposit. The measurements were performed well behind the trench wall, in order to avoid exposure of the deposited snow to air. For avalanche #3 the temperature was measured with the vertical probes and measurements were started simultaneously from both sides of the avalanche. Additionally the center profile (Pdepo) was performed at the same time. This took about 1-2 hours in total. A single measurement with the temperature probes took about 3-5 minutes. The depth of the debris could be well observed as a sharp temperature gradient in the temperature measurements itself. To verify this, a trench or regularly spaced pits were dug and the interface between debris and undisturbed snow cover was identified.

2.3.3 Calculating mass RC: It is not clear to me how the mass was calculated for avalanche #2 since the laser scan is only partly available (Table 1).

AC: Unfortunately the laser scan before the release did not cover the entire avalanche area. Nevertheless, field observations (Figure 1b) showed that the avalanche entrained the same snow layers along the path. We therefore extrapolated the TLS measurements from the upper part of the entrainment area of TLS data to the lower part until the elevation where the deposits started.

3 Technical comments RC: Fig 1c: step down not visible.

AC: Changed terminology to secondary release.

RC: Fig. 2: avalanche #4 is #3, I assume?

AC: The legend has been changed accordingly

RC: Fig. 3 and 5: Please export the infrared data into an external program to avoid plotting unnecessary information and to provide more temperature values in the color bar. This also helps to avoid using colors in the text instead of values (“from pink to orange”, p5862 line 6), or a change in the temperature scale. AC: Figure 3 and 5 are compressed videos and therefore do not allow to be processed as raw data in an external program. As indicated in the caption of the figures the presented images are screenshots from the videos.

RC: Fig. 4: Please mention in the caption and in the text to which avalanche this data belongs

AC: We have added the requested info.

RC: Fig. 6a: The transects appear to me that they did not extend into the undisturbed snow, while this is indicated in Figure 7. AC: This is now better illustrated in Figure 6.

RC: Fig. 6c: The transect appear to be not on the avalanche (bad angle). This transect was not used in Fig. 7, so this figure could be deleted.

AC: This is correct. The figure was removed.

RC: Fig. 8: Please enlarge the axes labels.

AC: Adapted as suggested.

RC: P. 5799, line 8ff. The authors could verify with the available laser scanning data if the entrainment in the gullies was indeed negligible.

AC: TLS measurements were not performed for the upper part of the rock face since the gullies would cause a lot of areas which are shaded from the measurements. Due to the steepness of the terrain (all above 45°) which causes constant avalanching and the very small potential entrainment area in the gullies the mass contribution can be assumed to be small compared to the snow in the slope below the rock face.

RC: P. 5802, line 15ff: The reasonable relation between temperature and erosion depth could be investigated with laser scanning data or measurements of the crown height.

AC: In fact this can exactly be observed for the release area of avalanche #2 when comparing the TLS data in Figure 2 (larger release depth) with Figure 6b (warmer snow surface temperatures).

RC: P. 5805, line 9ff: Please discuss why you think the 1.5 deg is an upper limit. If additional mass is entrained, more potential energy is available, which will increase deltaT, while early deposition of mass on the track does the opposite. Do the authors think early deposition dominates?

AC: We have now corrected this conclusion. See also answer to comment "1.2 Evaluation of the overall quality". Our initial calculation assumed that the entire mass, i.e. the released and entrained mass, is concentrated at the elevation of the release area. This is an extreme case in the sense that, normally, (large) parts of the mass is entrained along the path, lowering the center of mass, and thus providing less potential energy that can be transformed into heat. We now stick more to our avalanche situation and we calculate the friction contribution using the real centre of mass, providing a more

detailed mass- and elevation-dependent calculation as discussed in detail above. Early deposition does for sure not dominate for the observed avalanches. Both avalanches exhibit a pronounced growth index.

RC: P. 5806, line 10ff: Do the authors mean "altitudinal changes" (gradients) are variable, or temperatures are variable due to an altitudinal gradient.

AC: We intended to indicate that snow temperatures can be variable due to an elevation gradient, with warmer snow temperatures typically at lower elevations. This has been shown in the cited paper of Steinkogler et. al, 2013). We reformulate this in the paper to be more understandable.

RC: P. 5806, line 19ff: I suggest to consider that warmer temperatures at the bottom of the flow could be explained with upper layers were cooling faster due to enhanced air contact. The authors have used similar arguments at the lowest deposition layers which cooled to the temperature of subjacent snow.

AC: Cooling in the uppermost areas of the deposits has to be expected and was accounted for. Gray areas in Figure 9 indicate the areas of the snow profiles which where neglected (both on the top and at the bottom of the deposits) to account for temperature changes. Yet, we do not expect that the snow at depths of approximately more than 30cm below the surface experienced a significant cooling the relatively short time between the avalanche stopping and the measurements.

RC: P. 5806, line 24: Please explain why this shape of the temperature profile indicate plug like flow.

AC: We have used the wrong terminology. We did not mean to extrapolate the flow regime from the temperature profile but we wanted only to recall that the shape of the temperature profile resemble the one of a plug flow. This is not the correct word in this context. We will change the text accordingly and we will suggest that the constant temperature in depth may rather indicate a good mixing of snow in the avalanche core.

It is not possible to draw conclusions on the temperature profile shape at the boundary conditions (top/bottom) of profile, since cooling/warming effects from air and basal snow layer (gray areas in Fig. 9) may have corrupt the measurements.

RC: P. 5809, line 1: “Deposits from the powder cloud have consistently lower temperatures ...” Consider more careful wording, since only three avalanches were studied and it is not clear if the powder cloud and the dense core can easily be discriminated in the infrared images.

AC: As suggested we reword this statement.

Interactive comment on The Cryosphere Discuss., 8, 5793, 2014.

The Cryosphere Discuss., 8, C3215–C3219, 2015
www.the-cryosphere-discuss.net/8/C3215/2015/

The Cryosphere
Discussions
Open Access

Interactive comment on "Thermal energy in dry snow avalanches" *by* W. Steinkogler et al.

W. Steinkogler et al.

steinkogler@slf.ch

Received and published: 19 March 2015

We would like to thank the reviewer for the constructive comments, which also refer to many points of reviewer 1 and especially to a better discussion on the separation of thermal sources due to friction and entrainment.

GENERAL COMMENTS: The paper address an important issue in avalanche dynamics, as, how the authors state, recent investigation showed that the temperature of the moving snow is one of the most important factors controlling the mobility of the flow. Starting form an experimental approach, collecting data on real avalanche events, the authors propose then a method to calculate the thermal balance in the avalanches, from release to deposition, identifying two main sources of thermal energy: friction and entrainment. They also discuss the application of the IRT technique to investigate the thermal properties of the avalanches.

RC: The paper is well written and structured and the reader can easily follow all the story, from data to results, with good figures. The discussion section is a bit unbalanced towards the applicability of the IRT technique, while from the abstract and the rest of the paper, it seems that the main aim is the evaluation of the thermal energy of an avalanche (p. 5796, ll. 9-11).

AC: We restructured parts of the paper to account for this reviewer statement. We also added more detailed technical information in the IRT technique in the methods section as requested by reviewer 1.

As I agree with the detailed revision of the other reviewer, I will not write in the following again the same points, but just expand some concepts and add some more specific comments. In particular, I think the main point which need to be discussed better is the identification of the contributions to the thermal energy increase from friction and entrainment, which the authors identify as separate ones. Finally, I think that the paper is ready for publication after major revisions.

SPECIFIC COMMENTS: RC: p. 5793, ll. 13-19 (and later in the manuscript): how can you state this? Can you really separate the two contributions? The statement related to the importance of the elevation drop for the warming due to friction is too much general. Starting from only three avalanches on the same slope I would not generalize the results. I would present the results in a less general way. It is already a good result the presentation of what you could measure with field work and IRT technique. The attempt of explaining the thermal energy increase in a general way is ambitious and valuable but I think it needs more work (and data).

AC: We agree with the reviewer and will moderate our conclusions and now a more detailed analysis has been introduced. See comment 1.2. and 2.1.2. from reviewer 1.

RC: p. 5796, l. 9-13: Here you describe the aim, where the emphasis is put on the quantification of the thermal energy in avalanches. As in the discussion you then put more emphasis in the IRT stuff, I would here write something like "A secondary aim is

to evaluate the application of the IRT technique to get deep insights into the thermal state of an avalanche". The last sentence (ll. 12-13) is not an aim. I would keep this last paragraph of the Introduction only to clear state the aims of the study.

AC: We did as suggested.

RC: p. 5797, ll. 19-22: which is the spatial resolution of the measurements? Fig. 8 shows continuous values, which are an interpolation of the measurements. The grid should be presented or at least this information given. And, is the profile georeferenced and matched with the laser scan measurements? In general, how did you match the point data, the profile data and the grid data of IRT and TLS?

AC: The requested information has been added to the paragraph 2.4. Information on geo-referencing and matching of the data can be found in the response to comment 2.1.3. of reviewer 1.

RC: p. 5798, ll. 25-27: here you state that laser scan was used for the determination of the release and erosion depths along the track, and later (p. 5800, l. 21 and p. 5801, l. 11) you report values for the deposition masses. In general, keep in mind that laser scan can only give information on the net volume difference between erosion and deposition. It is not the topic of this paper, but I would discuss this, as you need the mass for your calculation. I would also give the value of the density of the deposit, which I guess you used, together with the deposition volume from laser scan, to calculate the deposition mass.

AC: We agree with the reviewer and are aware of this fact. We calculate the released and entrained mass by combining the TLS information with density information from snow profiles. This was then summed up to estimate the deposition mass. In addition to Table 1 we will provide values of the density measurements for release, entrainment and deposition are in the text.

RC: p. 5802, Section 4.1.1: you write about avalanche #1 and #2 and not #3? Is there

a reason? For completeness I would describe also the third avalanche.

AC: Unfortunately no good IRT data is available for the motion of avalanche #3 due to a cloud that moved in during the avalanche release. IRT data is only available as the avalanche comes to a stop and afterwards.

RC: p. 5082, ll. 22-25: I would not state that lateral IRT profile allowed to differentiate between undisturbed snow cover, dense core and the deposits of the fluidized layer. The limits are not so clear. I would say that comparing the IRT data with field observations you could identify the three zones where surface snow temperature are different. Otherwise, as it is written now, it seems that in general the IRT technique could be used to identify the deposit of different parts of an avalanche (dense and fluidized layers). More avalanches should be analysed to be able to propose a generalized methodology suitable to this aim.

AC: We agree with the reviewer that this statement is too general. Additionally we changed the term "fluidized layer" to "thin deposit area" as we cannot show with measurements that this layer existed inside the avalanche. See response to comment 2.2. of reviewer 1 for more details.

RC: p. 5805, ll. 4-5: I think that you cannot drop the mass m in eq. (3), as you yourself in the previous section (4.2.2) wrote that entrainment is happening...

AC: We now provide a more detailed and mass dependent calculation. See response to comment 1.2. of reviewer 1 for more details.

RC: p.5804, ll. 23-24: explain better how you can say that the profile temperature can give information related to the type of avalanche regime (plug-like flow).

AC: The terminology was incorrect and this part was changed accordingly. See comment of reviewer 1 related to P. 5806, line 24 for more details.

RC: Table 1. Which density value you used to calculate the mass? I would add this info in the caption.

AC: We added this information to the text.

Interactive comment on The Cryosphere Discuss., 8, 5793, 2014.

Manuscript prepared for J. Name
with version 2014/05/22 6.83 Copernicus papers of the LaTeX class copernicus.cls.
Date: 1 May 2015

Thermal energy in dry snow avalanches

Walter Steinkogler[1,2], **Betty Sovilla**[1], **and Michael Lehning**[1,2]

[1]WSL Institute for Snow and Avalanche Research SLF, Davos Dorf, Switzerland
[2]CRYOS, School of Architecture, Civil and Environmental Engineering, EPFL, Lausanne, Switzerland

Correspondence to: Walter Steinkogler (steinkogler@slf.ch)

Abstract. Avalanches can exhibit many different flow regimes from powder clouds to slush flows. Flow regimes are largely controlled by the properties of the snow released and entrained along the path. Recent investigations showed the temperature of the moving snow to be one of the most important factors controlling the mobility of the flow. The temperature of an avalanche is determined by the temperature of the released and entrained snow but also increases by frictional ~~and collisional~~ processes with time. For three artificially released avalanches, we conducted snow profiles along the avalanche track and in the deposition area, which allowed quantifying the temperature of the eroded snow layers. ~~Infrared radiation thermography (IRT) was used to assess the surface temperature before, during and just after the avalanche with high spatial resolution.~~ This data set allowed to calculate the thermal balance, from release to deposition, and to discuss the magnitudes of different sources of thermal energy of the avalanches. ~~We could confirm that, for~~ For the investigated dry avalanches, the thermal energy increase due to friction was mainly depending on the elevation drop of the avalanche with a warming of approximately ~~0.5~~0.3C per 100 height meters. Contrary, warming due to entrainment ~~was very specific to the individual avalanche~~ varied for the individual avalanches, from 0.08 to 0.3C, and depended on the temperature of the snow along the path and the erosion depth~~ranging from nearly no warming to a maximum observed warming of 1C. Furthermore, we could observe the warmest temperatures are~~ . Infrared radiation thermography (IRT) was used to assess the surface temperature before, during and just after the avalanche with high spatial resolution. This data set allowed to identify the warmest temperatures to be located in the deposits of the dense core. Future research directions, especially for the application of IRT, in the field of thermal investigations in avalanche dynamics are discussed.

1 Introduction

Avalanches can exhibit many different flow regimes (Gauer et al., 2008) depending on 1) the released and entrained amount of snow, 2) the properties of the snow and 3) the topography (slope, curvature) (Naaim et al., 2013). Studies showed that avalanches can increase their mass due to entrainment by multiple factors (Sovilla et al., 2007; Bates et al., 2014) which in turn influences the run-out distance. Even though important, the amount of snow entrained is not the main controlling factor that determines the flow form of the avalanche (Bartelt et al., 2012). The flow regimes and in turn mobility are strongly influenced by the properties of the entrained snow (Steinkogler et al., 2014b). Data on front velocities, run out, flow regimes and powder clouds revealed that different avalanches can form with similar release conditions and on the same avalanche path depending on the inherent snow cover properties. Advancements in avalanche dynamics models allow to account for the properties of the flowing snow with more and more detail (Valero et al., 2015) .

Recently, it has been shown that snow temperature inside an avalanche can significantly change its flow dynamics (Naaim et al., 2013; Steinkogler et al., 2014b), mainly by changing the granular structure of the flow (Steinkogler et al., 2014a). Laboratory studies on the granulation of snow showed a distinct dependency on snow temperatures with a fundamental change in snow structure at a threshold of -1C. Therefore, significant changes in flow dynamics can be expected with relatively small changes in temperature around this threshold.

Measuring temperature inside a flowing avalanche or in its deposit with traditional methods has proven to be difficult due to technical constraints or because measurements can not be conducted due to safety reasons. In addition to manual snow profiles we therefore investigate the application potential of infrared radiation thermography (IRT) technologies.

IRT is a non-contact, non-intrusive technique, which enables us to see surface temperature in a visible image. Meola and Carlomagno (2004) give an overview on existing work and describe the most relevant industrial and research applications of IRT.

The emissivity of a surface is a function of many factors, including water content, chemical composition, structure and roughness (Snyder et al., 1998) as well as the viewing angle between observer and measurement object. Even though many technical challenges and shortcomings of IRT are known, possible applications on the field of snow science have recently been discussed (Shea and Jamieson, 2011). Shea et al. (2012) and Schirmer and Jamieson (2014) applied IRT to measure spatial snow surface temperatures on snow pit walls. It was found that fast and large temperature changes resulting from surface energy balance processes must be expected (Schirmer and Jamieson, 2014). These energy balance processes between air and snow are particularly important during windy conditions, clear skies and large temperature differences between air and snow. These findings indicate that measuring the snow surface temperature of avalanche deposits or erosion layers along the track must be carried out as fast as possible. IRT can therefore be seen as a useful qualitative tool for snow applications whose quantitative operation still needs further verification.

The aim of this study is to identify the spatial temperature distribution in an avalanche and to quantify potential sources of thermal energy in an order of magnitude estimation. This is achieved by field measurements and the application of an IRT camera. ~~Furthermore, the acquired IRT videos allow to observe the avalanche phenomenon from a mainly qualitative but nevertheless unique point of view.~~ A secondary aim is to evaluate the application of the IRT technique to get deeper insights into the thermal state of an avalanche.

2 Methods & Data

2.1 The Flelapass field site

Multiple dry avalanches were artificially released during winters 2012-13 and 2013-14 at the Flelapass field site above Davos (Switzerland). Here we will discuss three avalanches, #1 (23 January 2013), #2 (05 February 2013) and #3 (31 January 2014), out of this data base (Fig. 1).

The avalanche path is a north-east facing slope covering 600 vertical meters. Deposits of larger avalanches typically reach a lake located at 2374 m a.s.l. at the bottom of the slope (Fig. 2). Observations and remote measurements can safely be conducted from the road at the pass which is approximately 800 m away from the avalanche. The slope angle ranges from 50 in the rock face in the upper part to 20 at the beginning of the run-out zone with an average of 30 of the open slope around 2600 m a.s.l..

2.2 Snow profiles

To assess the properties of the released and entrained snow, manual snow profiles according to Fierz et al. (2009) were conducted in the release zone ($P_{release}$), i.e. just below the rock face, along the track (P_{track}), in the deposition zone (P_{depo}) and in the undisturbed snow cover in the run out zone (P_{runout}) (Fig. 2). The profile location of the initially released cornice is refereed to as $P_{cornice}$. In combination with release and erosion depths, the acquired snow profiles allowed to identify which layers were entrained into the avalanche.

All profiles were conducted as fast as possible after the avalanche stopped. Yet, especially for the profiles in the release area and the track, it took around 30 minutes to reach the profile locations. The temperature measurements close to the surface must therefore be interpreted carefully due to a rapid adaptation to the ambient conditions.

In addition to the acquired video and pictures of the powder cloud the deposits of the avalanche were investigated for indications of different flow regimes according to the observation criteria of Issler et al. (2008) .

2.3 Lateral temperature profiles

In addition to the regular snow profiles, trenches were dug in the deposition zone and modified avalanche probes were used to measure lateral temperature gradients. The modified temperature probes (BTS) are regular avalanche probes for which the tip was replaced by a thermistor. BTS probes are usually used for permafrost applications (Lewkowicz and Ednie, 2004; Brenning et al., 2005) to measure the temperature at the interface between soil and snow. Their application allowed to measure the temperature of snow layers without exposing them to the ambient air temperature. As for the thermometers used for regular snow profiles (Section 2.2) they measure the snow temperature with an accuracy of $\pm 0.1°C$. As for the regular snow profiles the upper most layers need to be interpreted carefully in this investigation due to an expected change in temperature over time.

The lateral temperature measurements were conducted to the left and right side of snow profile P_{depo}, which was situated in the center of the deposition zone (Fig. 2). Every BTS measurement took around 3-5 minutes. The interface between deposits and the undisturbed snow cover underneath could be identified in a rapid gradient in the temperature measurements. The snow depth of the deposits was determined by regularly spaced pits along the transect after the temperature measurements.

2.4 Infrared radiation thermography (IRT) camera

The snow temperature measurements acquired from profiles where supplemented with an infrared radiation thermography (IRT) camera which allowed to record snow surface tem-

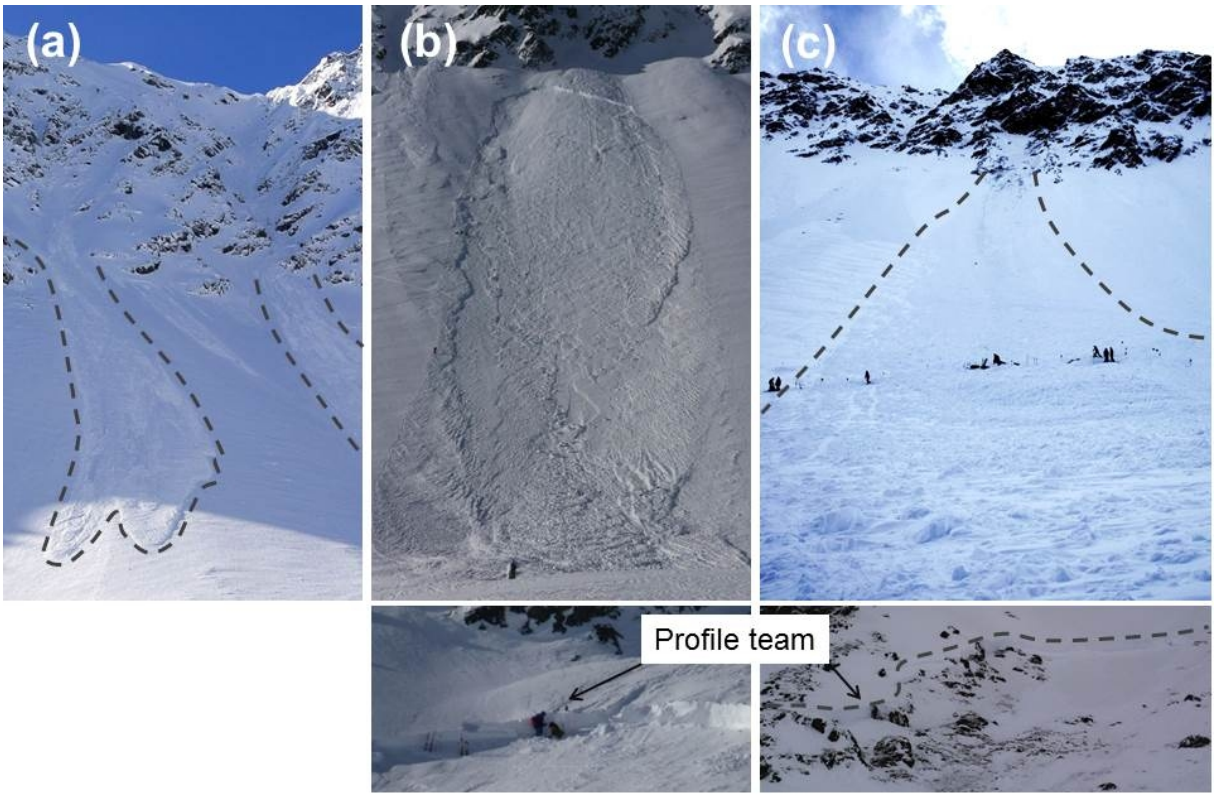

Figure 1. Avalanches at the Flelapass field site released by artificial triggering of the cornices on the ridge. Avalanche #1a and #1b (a) were released on 23 January 2013, #2 (b) on 05 February 2013 and #3 (c) on 31 January 2014. Note the significant ~~step-down~~ secondary release and entrainment of deeper layers below the rock face for (b) avalanche #2 and (c) avalanche #3.

peratures before, during and after the avalanche (Fig. 3 and 5). Time-lapse measurements after the avalanche stopped allowed to follow the temporal evolution of surface temperatures (Fig. 4) and videos of the moving avalanche provided a qualitative yet illustrative point of view (provided as supplementary material). The first pictures were recorded as fast as possible (usually less than 1 minute) after the powder cloud disappeared and the video recording was stopped.

We used an InfraTec VarioCAM hr 384 sl and a VarioCAM HD 980 s that both operate in the long wave infrared spectral range (LWIR) covering 7.5 to 14 μm. According to the manufacturer the cameras measure with an absolute accuracy of $\pm$1.5C and a resolution of 0.05C. The measurements were either conducted with a 15 mm or a 30 mm lens. With the used IRT cameras and lenses the pixel size of the footprint is approximately 1 m with the old camera and 0.5 m with the newer model. Since cold and dry atmospheric (determined by an automatic weather station close by) and snow conditions prevailed during all conducted avalanche experiments an emissivity value of 1 has been chosen for all post-processing operations.

Even though in our study we use the IRT measurements mainly in a qualitative way, a basic verification was conducted. The snow surface temperatures recorded with the IRT camera (solid lines in Fig. 4) were compared to manually measured snow surface temperatures (dots in Fig. 4) at the corresponding snow profile locations (Fig. 2). The snow surface temperatures of the release ($IRT_{release}$) was compared to the corresponding layer in the snow profile in the undisturbed snow ($T\_P_{release}$ at 0 min) and measured surface temperatures with a digital thermometer ($T\_P_{release}$ at 45 min). The same was conducted for the surface temperature along the erosion layer in the avalanche path (T_P_{track}). Both measurements are in fairly good agreement with an absolute difference of about ~~plus/minus~~ $\pm 1°C$.

2.5 Terrestrial laser scan (TLS)

A terrestrial laser scanner (Riegl LPM-321) was operated from the Flelapass road (Fig. 2) to acquire digital surface models before and after the avalanche releases. The measurements facilitated the calculation of the release and erosion depths along the path. A complete set of terrestrial laser scans is available for avalanche #3 only. For avalanche #2 the scan before the avalanche is only available for the release zone (Fig. 2). No information from terrestrial laser scanning was available for avalanche #1. Avalanche boundaries and field measurement locations were recorded by GPS allowing spatial referencing with the TLS data. The

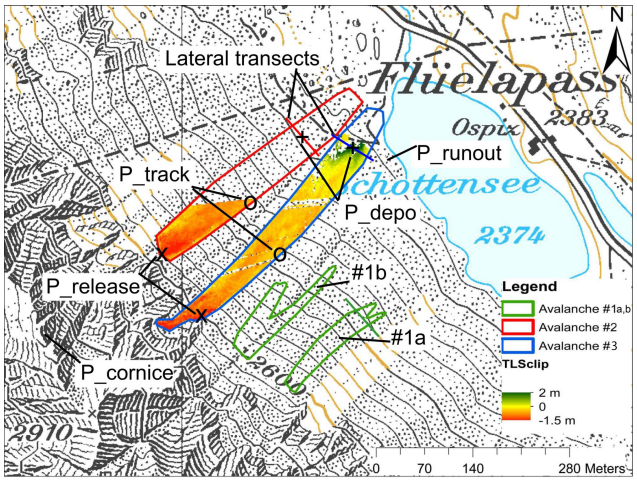

Figure 2. Flelapass field site close to Davos (Switzerland). Outlines of avalanche #1a and #1b (green), #2 (red) and #3 (blue). The colorbar shows differences between terrestrial laser scans before and after the individual avalanches. $P_{release}$ and P_{track} indicate locations of snow profile in the release and along the path, respectively. Red and blue lines indicate positions of lateral investigations and deposition snow profile P_{depo}.

underlying (summer) digital elevation model was available with 1 m spatial resolution.

3 Investigated avalanches

This section summarizes the key characteristics and available data (Table 1) of the avalanches. All avalanches were released after a snow storm by triggering the cornices at the ridge at 2900 m a.s.l. with explosives. Therefore, most of the released snow was new snow. Yet, two of the avalanches, avalanche #2 and #3 (Fig. 1b and c), entrained significant amounts of snow from deeper layers due to a ~~step-down, i.e. a secondary release to~~ secondary release in a deeper weak layer, below the rock face. Since the main mass contribution can be assumed to be defined by the secondary releases ~~below the rock face~~ and the entrainment along the path, we focused our investigations on these snow masses. Mass contributions by the cornices are usually relatively small compared to entrained snow on the open slope below. Furthermore, entrainment of snow in the gullies of the rock face is not assumed to contribute a significant amount since regularly occurring (small) avalanches and slides continuously erode the snow cover. In this study we use the word release to refer to profile locations at the secondary release below the rock face (Fig. 2).

Avalanche #1a and #1b (23 January 2013):
In the days previous to the avalanche experiment 10 cm of new snow were recorded and snow drift accumulations formed due to strong southerly winds. The national avalanche bulletin reported a moderate avalanche danger (level 2) and identified the fresh snow drift accumulations as the main danger. During the experiment clear sky conditions prevailed and the automatic weather station (AWS) at the Flelapass (FLU2) measured an air temperature of -10C. Multiple charges were exploded on the ridge to the lookers-left (South) of the summit resulting in two independent small powder avalanches which followed the gullies (Fig. 1a and Fig. 3). Due to the relatively small release mass and no significant entrainment both avalanches, #1a and #1b, stopped half way down the open slope. Even though the avalanches were small and a full data set of field measurements is not available, they are retained in this study since they provide good quality IRT data (Fig. 3). We excluded the snow profile measurements from the analysis since the erosion and deposition depths were very small, around 0.1 m, and the manual measurements were conducted more than 1 hour after the release. The deposition zone was not accessible before due to safety reasons. The TLS could not be completed due to technical problems.

Table 1. Summary of measurements for the investigated avalanches. * indicate that erosion and deposition depths were too small. Growth Index I_g is defined as $I_g = m_e/m_r$.

Avalanche	**#1a**	**#2**	**#3**
Date	23 Jan. 2013	05 Feb. 2013	31 Jan. 2014
IRT camera model	hr 384 sl	hr 384 sl	HD 980 s
Terrestrial laser scan	no	partly	yes
Snow profiles lateral	-*	yes	yes
Snow profiles track	-*	yes	yes
IRT video	yes	yes	no
IRT pictures	yes	yes	yes
Released mass m_r (t)	-	502	818
Entrained mass m_e (t)	-	1857	1302
Deposited mass m_d (t)	-	2359	2120
Growth Index I_g	-	3.7	1.6

Avalanche #2 (25 February 2013):
20 cm of fresh snow that covered older snow drift accumulations resulted in a considerable (level 3) avalanche danger. Furthermore, the bulletin noted that avalanches in isolated cases could be released deeper within the snowpack. The AWS at Flelapass measured -12C and a partly cloudy sky prevailed during the experiment.

Explosions along the ridge and to the lookers-left (South) side of the summit only produced small avalanches that stopped shortly below the rock face. A single explosion that triggered the cornice to the right side of the summit caused another small powder avalanche that followed the gully and triggered a secondary release at the start of the

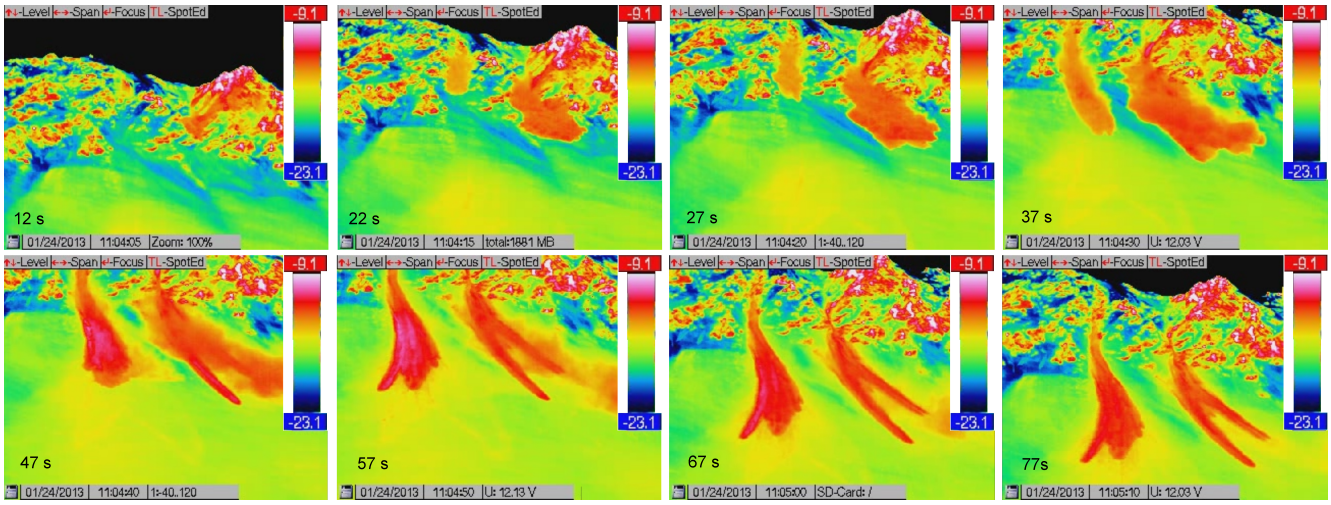

Figure 3. Screenshot of IRT camera videos for avalanche #1a and #1b. The first picture was taken 12 s after the avalanche released.

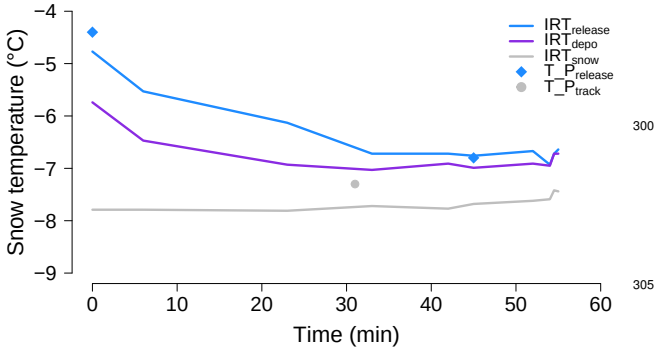

Figure 4. Temporal evolution and comparison of snow temperatures of avalanche #2 using a IRT camera and manually measured data. Solid lines represent regular IRT measurements in the release ($IRT_{release}$), the deposition area (IRT_{depo}) and the undisturbed snow cover (IRT_{snow}) which are compared to manual measurements at the profile locations ($T\_P_{release}$ and T_P_{track}).

open slope (Fig. 1b). Even though the avalanche almost stopped after entering the open slope, the additional mass which was entrained resulted in an re-acceleration resulting in a long running medium-sized avalanche (deposition mass 2357 t) which only stopped in the flat part close to the lake. Average snow density of the release was 170 $kg\,m^{-3}$ and 210 $kg\,m^{-3}$ for the entrained snow. No full TLS was available before the avalanche release. Nevertheless, in-field observations showed the entrainment depth to be rather homogenous along the slope which allowed to extrapolate the upper entrainment area and thus to calculate the entire entrained mass.

Avalanche #3 (31 January 2014):
Multiple consecutive smaller snowfalls and strong southerly winds created snow accumulations close to ridges. The national avalanche bulletin issued a considerable (level 3) danger level and that the weak old snowpack could cause avalanches to be released in near-ground layers. Moderate winds with gusts up to 60 km/h from the South and cloudy to overcast conditions prevailed during the experiment. The automatic weather station FLU2 recorded -6C with steadily increasing temperatures during the experiment.

Two small spontaneous avalanches already released before the experiment. Initial bombing of the main gully and to the lookers-left (South) of the summit did not produce any significant avalanches. Yet, the bombing of the cornice to the lookers-right (North) of the summit resulted in a small powder avalanche which triggered a second slide at the lower end of the rock face (similar to avalanche #2). Consequently a significant amount of snow was eroded and resulted in a medium-sized avalanche (deposition mass 2120 t) that stopped in the flat run out zone (Fig. 1c). The secondary release nearly entrained all layers to the bottom of the snowpack (1.6 m). Average snow density of the release was 270 $kg\,m^{-3}$ and 310 $kg\,m^{-3}$ for the entrained snow. For avalanche #3 snow temperature measurements were also available for the cornice at the ridge.

4 Results

Based on these measurements we present observed temperature distributions during the avalanche motion as well as at the surface and inside the deposition zone (Section 4.1). In a second step potential sources of thermal energy are identified and quantified (Section 4.2).

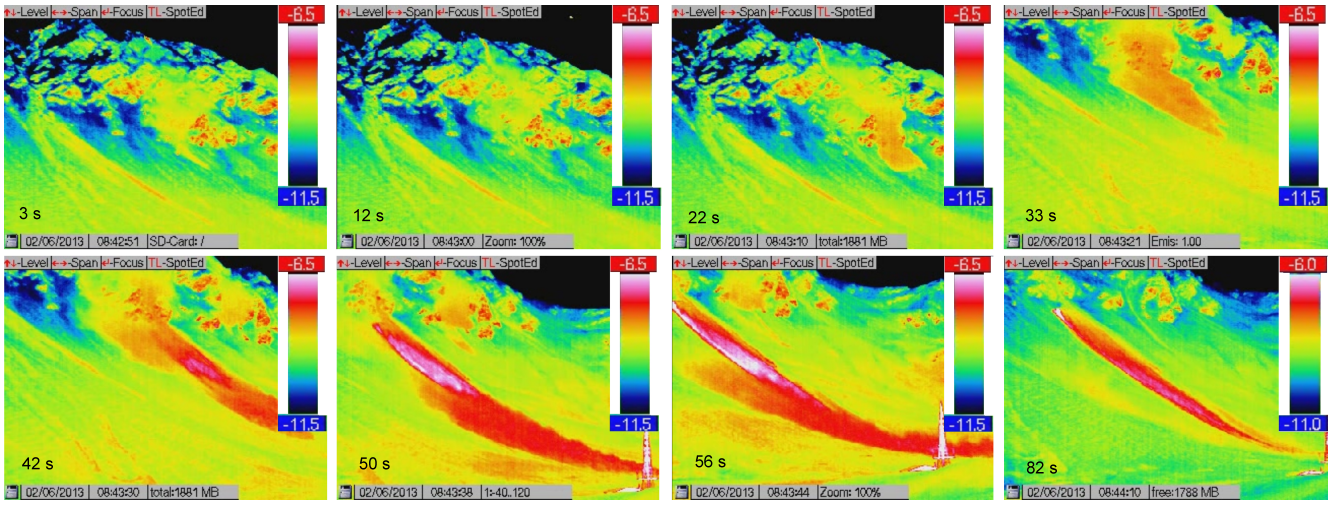

Figure 5. Screenshot of IRT camera videos for avalanche #2. The first picture was taken 3 s after the avalanche released. Note that the temperature scale was changed by 0.5C for the last shown image (82 s).

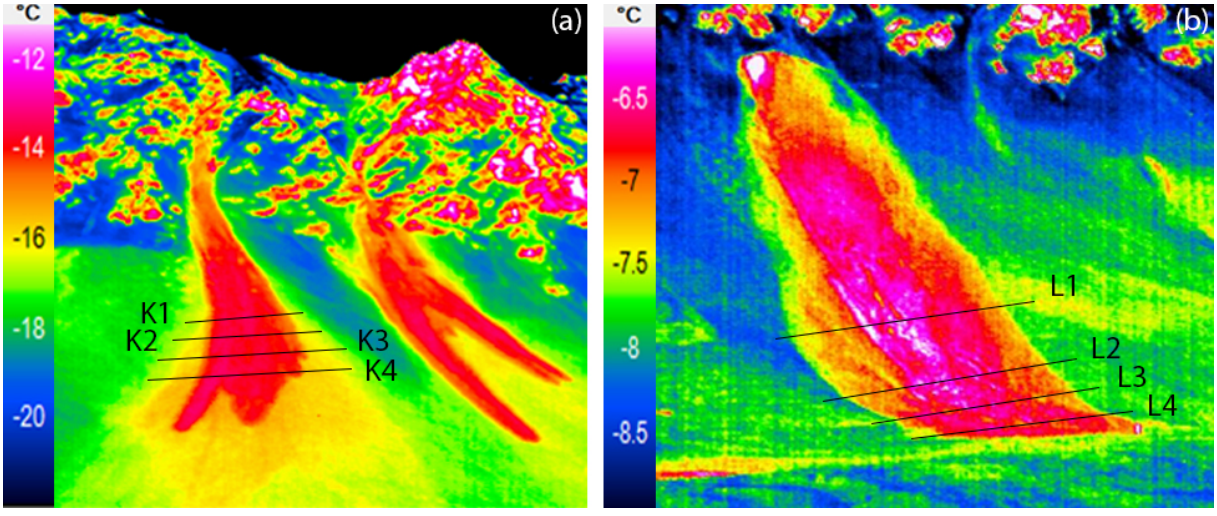

Figure 6. IRT camera images for avalanches (a) #1a and #1b ~~,~~ and (b) #~~2 and (c) 3.~~ 2. Note the different temperature scales amongst the avalanches. Black lines indicate positions of lateral snow temperature transects~~and profiles~~.

4.1 Temperature distribution

4.1.1 Avalanches in motion

The use of the IRT camera gave very interesting qualitative insights into the temperature behavior of a moving avalanche (Fig. 3 and 5). Especially plume formation, entrainment of warmer snow and the stopping of the avalanche as the powder cloud starved and drifted aside could be very well observed. (See supplementary material for the videos).

Even though avalanche #1a was small, a significant powder cloud developed shortly after the release (Fig. 3). After the avalanche entered the open slope (37 s), plume formation stopped, accompanied by a visible decrease in velocity, and the powder cloud drifted to the up-hill looking right side (47 s) due to the prevailing wind, revealing the until then obscured dense core (57 s). After that a rapid cooling of the surface of the dense core could be observed (from pink colors at 57 s to orange at 77 s).

The IRT video of avalanche #2 (Fig. 5) is of special interest since a distinct acceleration of the avalanche can be observed as it approaches the open slope below the rock face (33 s). This can be explained by the entrainment of mass of the secondary release (42 s). The powder cloud shows higher temperatures than during the first phase (50 s) and the eroded surface becomes visible after the powder cloud drifts aside (56 - 82 s).

4.1.2 Surface temperature distribution

The IRT camera images acquired shortly after the avalanches stopped (Fig. 6) allowed to identify exposed deep, and thus warmer, layers in the release and along the path as well as in the deposited snow. In Fig. 6b the secondary release, below the steep rock part, showed a much deeper erosion in the, looking up-hill, left corner. In the lower part of the track erosion was spatially rather homogenous for all avalanches.

Lateral IRT surface temperature transects in the deposition area of avalanche #1 and #2 (black lines in Fig. 6) revealed that the warmest part of the avalanche is located in the center and therefore in its dense core (Fig. 7a and c). In both cases a distinct difference in surface temperature of multiple degree Celsius between undisturbed snow cover and warmer core of the avalanche is evident. Figure 7b shows lateral profiles (L1 and L2 in Fig. 6b) along the path of ~~avalanche and allowed to differentiate between~~ the avalanche. These coincide with in-field measurements of the undisturbed snow cover, ~~the deposits of a fluidized~~ a thin-deposit layer that formed at the lookers-left (South) side of avalanche #2 and the dense core.

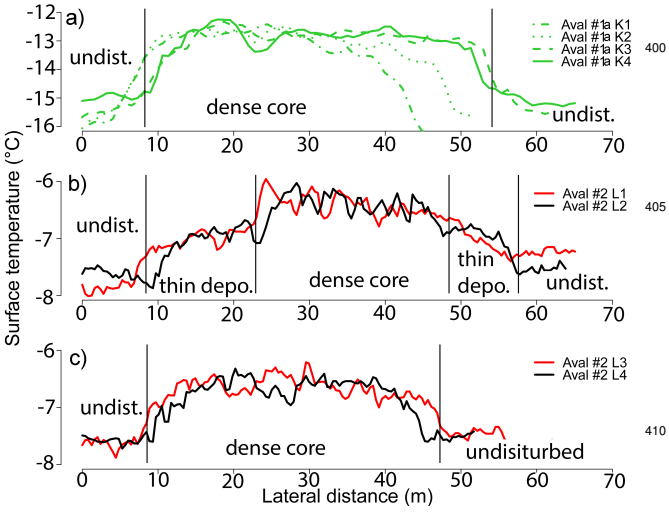

Figure 7. Snow surface temperatures acquired with IRT along lateral transects for avalanche #1 (a) and in the path (b) and the deposition area (c) of avalanche #2. Extent of undisturbed snow cover, ~~area of fluidized layer~~ thin-deposit and dense core are indicated. The lateral distance was calculated by referencing with the measured width of the avalanche.

4.1.3 Internal temperature distribution of deposits

The observed maximum temperatures in the dense core area did not only exist on the surface in lateral extension (Fig. 7) but also vertically in the deposits. This could be measured for both avalanches for which lateral investigations were conducted. Figure 8 shows the lateral temperature measurements conducted in the deposition zone of avalanche #2 and #3. Measurement P_{depo}, corresponding to 0 m, was located in the middle of the deposition and marked the position of the full snow profile in the deposits (Fig. 2). Temperature measurement locations R and L were leading laterally from the center to the, looking uphill, right and left side of the avalanche deposits. Furthermore, the top of the avalanche deposits (solid line), the bottom of the deposits (dashed line) and the terrain (pointed line) are indicated. For better distinction the area of the undisturbed snow cover is additionally indicated by softened colors. Even though the transect shown in Fig. 8a only represents one half of the avalanche deposits from avalanche #2, the extent of the dense core (area between solid and dashed line) could clearly be observed in the measured snow temperature. Similar measurements were recorded for avalanche #3 where again the highest temperatures were recorded in the center of the deposits (Fig. 8b) with decreasing values towards the side of the deposits.

4.2 Thermal energy sources

To explain the observed ~~increased~~ increase in snow temperatures in the deposits of the investigated avalanches and to assign ~~and~~ an order of magnitude estimation of the sources of thermal energy, we ~~partitioned the total warming into~~ look at two important sources of energy, namely (i) friction and (ii) warming due to entrainment of snow~~and (ii) friction~~. Other potential sources of thermal energy, e.g. entrainment of air or adiabatic warming, were not ~~considered in this calculation since~~ further considered since an order of magnitude estimation revealed that their influence on the temperature of the dense core ~~were estimated as negligibly small and in the presented work~~is negligibly small (not shown).

4.2.1 ~~Entrainment~~

~~The snow profiles (see locations in Fig. 2) enabled a quantification of the properties of the released and entrained snow. Figure~~Figure 9 shows snow temperature profiles in the center of the deposition zone T_P_{depo} (solid violet line) and compares them to measurements conducted in the release zone $T\_P_{release}$ (blue line), along the path in the undisturbed snow T_P_{track} (orange) and the undisturbed snow cover in the run out zone T_P_{runout} (gray). ~~Comparing T_P_{depo} and $T\_P_{release}$ reveals that a significant warming took place.~~

~~Snow temperature measurements conducted in the release zone ($T\_P_{release}$), along the path in the undisturbed snow (T_P_{track}), in the undisturbed snow cover in the run out zone (T_P_{runout}) and in the deposition zone (T_P_{depo}) of (a) avalanche 2 and (b) avalanche 3. Release, entrainment and deposition depths are indicated by solid lines whereas the undisturbed snow cover is represented by pointed lines. Gray areas indicate parts of the temperature profiles that were neglected in the calculations because of expected changes in temperature over time due to the boundary conditions of the surface and the undisturbed snow cover. Composition~~

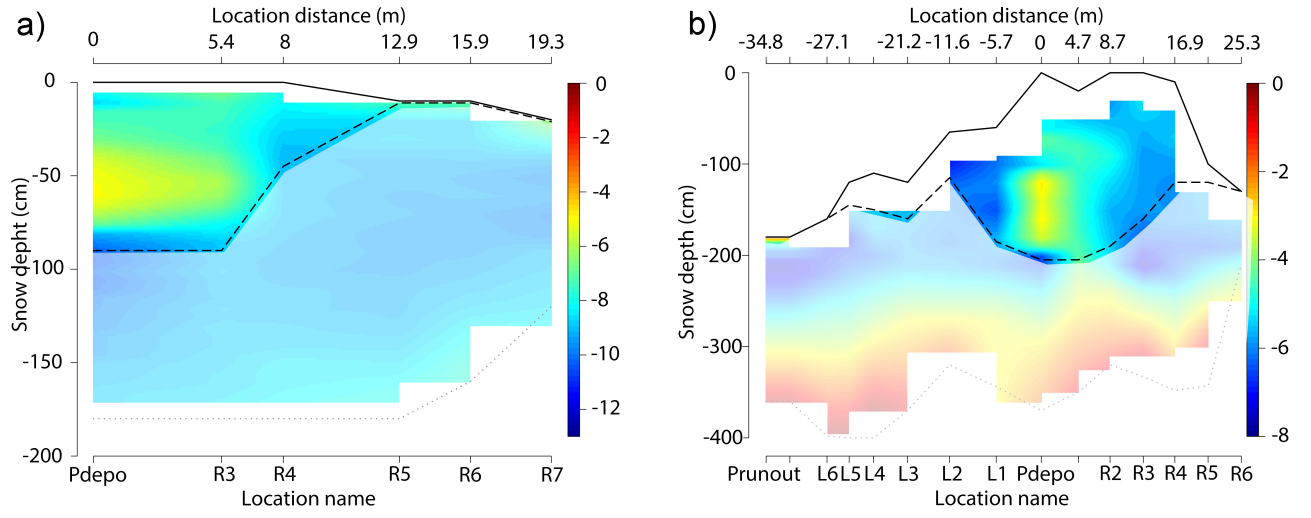

Figure 8. Lateral snow temperature profiles in the avalanche deposits of (a) avalanche #2 and (b) avalanche #3. P_{depo} and 0 m indicate the center of deposits and the index L and R represent left and right, looking uphill, measurement locations towards the lateral sides of the avalanches. Lines indicate the top of the avalanche deposit or snow cover (solid), bottom of avalanche deposit (dashed) and bottom of snow cover (pointed). Colors of undisturbed snow cover were softened for better distinction with avalanche deposits.

~~of deposits (granules and fine grains) are indicated for avalanche 2.~~

Depth-averaging the deposition profile (violet line in Fig. 9) yielded a snow temperature of -6.8C for avalanche #2 and -4.1C for avalanche #~~3.~~ 3 ($\overline{T\_P}_{depo}$ in Table 2). Temperature values from the upper and lowermost layers (0.2 m thick) were excluded from the calculations because of adaption of the temperature with the surrounding air and undisturbed snow cover (gray areas in Fig. 9). ~~Averaging, both spatially and vertically, the temperature for the snow that was released and entrained along the track results in -8.7~~Since $\overline{T\_P}_{depo}$ only represents the relatively warm core of the deposits we additionally calculated the mean of the lateral temperature profiles (Fig. 8) resulting in a mean temperature of the deposits $\overline{T}_{depo\_lateral}$ of -7.4C and ~~-5.8~~-4.8C for ~~the two avalanches (Table 2)~~avalanche #2 and #3, respectively.

Comparing the mean temperature of the deposits $\overline{T}_{depo\_lateral}$ with $\overline{T\_P}_{release}$ reveals that a significant warming took place. This resulted in a difference in snow temperature between ~~entrained~~ released and deposited snow of ΔT ~~1.9~~1.2C and ~~1.7~~1.5C for avalanche #2 and #3, respectively. ~~The temperature of the released and entrained snow could therefore not be the exclusive source of thermal energy.~~

~~Depth averaged temperatures of release ($\overline{T\_P}_{release}$), track ($\overline{T\_P}_{track}$) and deposition profile ($\overline{T\_P}_{depo}$) with the corresponding release and erosion depths (in brackets). The mean temperature $mean(T) = \overline{T\_P}_{cornice} + \overline{T\_P}_{release} + \overline{T\_P}_{track}$ in comparison to $\overline{T\_P}_{depo}$ results in the temperature difference between released and deposited snow ΔT which can not be explained by the entrained snow. **Avalanche 2 3** $\overline{T\_P}_{cornice}$ -5.3 C (1.05 m) $\overline{T\_P}_{release}$ -8.6 C (1.03 m) -6.3 C (1.75 m) $\overline{T\_P}_{track}$ -8.7 C (0.37 m) -5.8 C (0.3 m) $mean(T)$ -8.7 C -5.8 C $\overline{T\_P}_{depo}$ -6.8 C (0.9 m) -4.1 C (1.95 m) ΔT 1.9C 1.7C~~

4.2.1 Friction

The increase in temperature due to friction was calculated by assuming that all potential energy is transformed to heat. ~~Starting with potential energy~~

$$E_{pot} = m\ g\ h,$$

~~where m is the mass, g is the gravitational acceleration ($9.81\ m\ s^{-2}$) and h is the difference in elevation, we equated E_{pot} to the thermal energy E_{therm} resulting in~~ This means that the increase in temperature is only given by the drop height of the average avalanche mass:

$$E_{pot} = m\ gh = E_{therm} = m c_p\ \Delta T = m\ g \Delta h, \quad (1)$$

where m is the mass undergoing the change in potential energy, c_p is the specific heat capacity of snow (2116 $J\ kg^{-1}\ K^{-1}$)~~and ΔT~~, $\Delta T_{friction}$ is the change in snow temperature. ~~Solving for~~, g is the gravitational acceleration ($9.81\ m\ s^{-2}$) and Δh is the difference in elevation. Thus, ΔT ~~resulted in~~ is given by

$$\Delta T_{friction} = \frac{g\ h}{c_p} \frac{g \Delta h}{c_p}. \quad (2)$$

~~Note that m can be dropped if the massis not assumed to change along the path (i. e. no erosion or deposition takes place)~~This equation has general validity for any (incremental or finite) mass, in which potential energy is converted to heat. This is regardless of whether this mass is added to the avalanche by entrainment or whether it belongs to the initial release mass as long as Δh is the effective height drop of this mass. Calculating for an elevation drop of 300 m, corresponding to the slope below the rock face until the run out zone, ~~resulted in~~ we obtain an increase in temperature due to friction of approximately 1.5C.

The calculated $\Delta T_{friction}$ can be seen as ~~a maximum value~~ an upper limit in our order of magnitude estimation since in nature not all mass is released and entrained at the maximum elevation~~h~~. Furthermore, lateral temperature gradients in the deposition area are not taken into account. In practice avalanches entrain large portions of mass along the avalanche path. In many cases the entrained mass, m_e, is significantly larger than the released mass, m_r. This is also the case for the investigated avalanches which are characterized by a growth index of 3.7 and 1.6 for avalanche #2 and #3, respectively. If one further assumes that entrainment is happening uniformly along the path and that the vertical extension of the release area is small compared to the total path vertical drop, the entrained mass only experiences on average half the height drop of the released mass: $\Delta h_e = 0.5 \Delta h_r$. The effective Δh for Eq. 2 can then be calculated:

$$\Delta h = \frac{\Delta h_r \ (m_r + 0.5 m_e)}{m_r + m_e}. \tag{3}$$

For avalanche #2 and #3 this corresponds to a warming due to friction, $\Delta T_{friction}$, of 0.8 and 0.9 C, respectively.

4.2.2 Entrainment at a different temperature

The above development assumes that there is no difference between initial snow temperatures of the released and entrained snow. The snow profiles (see locations in Fig. 2) enabled a quantification of the properties of the released and entrained snow showing some difference as discussed above. Assuming that the entrained snow is completely mixed with the released snow in the deposition zone and that $\Delta T_{rel-ent}$ is this mean temperature difference between mass released and entrained, this difference leads to the following difference in temperature at the deposited snow mass:

$$\Delta T_{entrainment} = \frac{\Delta T_{rel-ent} \, m_e}{m_r + m_e}. \tag{4}$$

Since we assume that the heating due to friction is independent of the initial snow temperature either from release or entrainment, at least as long as the snow remains dry during warming, the temperature change due to a different snow temperature of the entrained snow can simply be added to the one from friction in Eq. 2. This results in a warming due to entrainment $\Delta T_{entrainment}$ of 0.08C and 0.3C for avalanche #2 and #3, respectively.

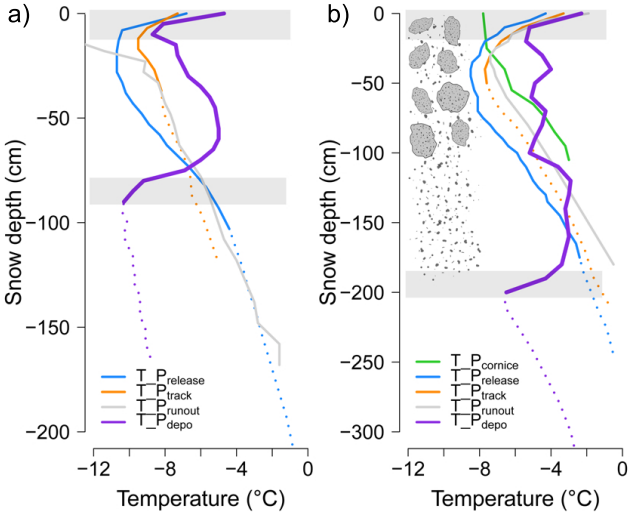

Figure 9. Snow temperature measurements conducted in the release zone ($T\_P_{release}$), along the path in the undisturbed snow (T_P_{track}), in the undisturbed snow cover in the run out zone (T_P_{runout}) and in the deposition zone (T_P_{depo}) of (a) avalanche #2 and (b) avalanche #3. Release, entrainment and deposition depths are indicated by solid lines whereas the undisturbed snow cover is represented by pointed lines. Gray areas indicate parts of the temperature profiles that were neglected in the calculations because of expected changes in temperature over time due to the boundary conditions of the surface and the undisturbed snow cover. Composition of deposits (granules and fine grains) are indicated for avalanche #2.

Table 2. Depth averaged temperatures of release ($\overline{T\_P}_{release}$), track ($\overline{T\_P}_{track}$) and deposition profile ($\overline{T\_P}_{depo}$) with the corresponding release and erosion depths (in brackets). $\overline{T}_{depo\_lateral}$ represents the mean of the lateral temperature measurements in the deposition. ΔT is the difference between $\overline{T}_{depo\_lateral}$ and $\overline{T\_P}_{release}$. $\Delta T_{friction}$ and $\Delta T_{entrainment}$ are the individual contributions to ΔT.

Avalanche	#2	#3
$\overline{T\_P}_{release}$	-8.6 C (1.03 m)	-6.3 C (1.75 m)
$\overline{T\_P}_{track}$	-8.7 C (0.37 m)	-5.8 C (0.3 m)
$\overline{T\_P}_{depo}$	-6.8 C (0.9 m)	-4.1 C (1.95 m)
$\overline{T}_{depo\_lateral}$	-7.4 C	-4.8 C
ΔT	1.2C	1.5C
$\Delta T_{friction}$	0.8 C	0.9 C
$\Delta T_{entrainment}$	0.08C	0.3 C

5 Discussion

It has been noted in other studies (Vera et al., 2012) that potential sources of thermal energy in snow avalanches are friction processes or entrainment of snow with differing temperatures. ~~Our results confirm that for the investigated avalanches~~ The investigated avalanches in this study indicate that the thermal energy increase ~~due to friction is mainly depending~~ was mainly defined by frictional heating, which in turn depends only on the elevation drop~~of the avalanche and thus a rather constant value (for a specific avalanche path and typology). The basic calculation does not take changes in mass into account.~~ . Yet, it is well known that avalanches can significantly increase their mass along the path via entrainment ~~(Sovilla, 2004) .~~ (Sovilla et al., 2006) . Also for the investigated avalanches the growth index were I_g of 3.7 and 1.6 for avalanche #2 and #3, respectively. Therefore, the calculated (maximum) value of 0.5C per 100 altitudinal meters (Eq. 2) has to be adapted to consider the actual mass that enters the avalanche at a certain point along the track (Section 4.2). For dry and cold snow avalanches far away from the melting point, the warming due to friction alone is ~~therefore~~ not expected to have a substantial influence on flow dynamics. Yet, if the overall avalanche temperature is already close to the critical temperature threshold of -1C (Steinkogler et al., 2014a) the warming by frictional processes can cause drastic changes of the granular structure inside the avalanche and consequently affect flow behavior.

Contrary, the warming due to entrainment ~~is very specific to the individual avalanche and can vary significantly depending on the~~ varied for the individual avalanches. These variations depend on the temperature of the snow and the erosion depth as shown in the profiles along the avalanche track (Fig. 9) and the IRT pictures (Fig. 6). ~~The~~ Typically, the alpine snow cover ~~typically~~ shows a positive temperature gradient towards the ground (Armstrong and Brun, 2008). Except for areas with permanent permafrost, the temperature at the soil-snow interface can be assumed to be approximately 0C if there has been a significant snow cover for several weeks. Consequently, the erosion of deeper snow layers leads to warmer snow temperatures ~~. Also altitudinal~~ (Fig. 9). Also changes of snow temperature ~~along the slope~~ due to elevation gradients have been proven to be quite variable and directly influence flow dynamics (Steinkogler et al., 2014b). Overall, the contribution of the temperature of the entrained snow to the warming was smaller than by friction for the investigated avalanches (Table 2).

Our temperature measurements on the surface (Fig. 7) and in depth (Fig. 8) of the ~~deposition zone~~ deposit indicate that the highest temperatures are located in the dense core of the avalanche. The interface between the bottom of the avalanche deposits and the subjacent undisturbed snow cover featured a very clear and sharp transition (violet lines in Fig. 9). The shape of the temperature curve indicates the warmest temperatures in the lower parts of the deposits profile (~~-40 to -80 cm and -120 to -190 cm~~ -0.4 to -0.8 m and -1.2 to -1.9 m for avalanches #2 and #3, respectively) and close to the sliding surface. This would support the expectation of the most pronounced friction at the bottom of the flow, typical for this kind of avalanche. Unfortunately, a cooling of the lowest deposition layers to the temperature of the subjacent undisturbed snow cover has to be expected and thus prevents a definite conclusion on this observation. ~~The upper part of the temperature profiles resemble more the shape of a plug-like flow.~~ Also, whether the small temperature variations in the upper part of the deposition profile between 0 and ~~-100 cm~~ -1 m of avalanche #3 (violet line in Fig. 9) are a result of a mixture of broken parts of the eroded snow cover, with varying temperatures, and formed granules could not be fully answered. Yet, granules embedded in fine grained snow were still clearly observable in this area of the deposition.

It is without question that reaching the deposits after an avalanche release to measure the snow surface temperature with traditional methods, e.g. thermometers, takes too long and the surface as well as the upper most layers would have changed their temperature already. It could be observed in the video of avalanche #1 (see supplementary material) that right after the dense core stopped it started to cool. In all those cases for which a real-time measurement is necessary IRT technology provides a valuable addition to traditional measurements. Even though in our study we only applied the IRT camera in a qualitative way, the presented basic verification (Fig. 4) with manually measured snow surface temperatures showed a fairly good agreement with an accuracy of about $\pm$1C. Although further investigations are necessary to define whether absolute values of surface temperature can be acquired without significant uncertainties, the relative accuracy of the IRT cameras are usually high, around 0.05C in our case as specified by the manufacturer. This facilitates to track relative changes in temperatures even if the absolute value might not be accurate.

Recently IRT was mainly tested and evaluated for snow profile applications at short distances (Schirmer and Jamieson, 2014). ~~Possible influences of the large distances between camera and avalanches, viewing angle, liquid water content in snow or at its surface (Snyder et al., 1998) and surface roughness of the deposits (Mushkin et al., 2007; Danilina et al., 2006) demand detailed studies. In general, low signal attenuation can be expected for (peak) winter month atmospheres, especially for clear sky conditions, due to relatively low humidity levels.~~

Dozier and Warren (1982) investigated the effect of viewing angle on the infrared brightness temperature of snow and found differences of up to 3C. Similar values have been found by Hori et al. (2013), yet they concluded that for viewing angles less than 40 from the nadir the error in temperature is less than -0.8C. The effect of moisture has been studied extensively (Wu et al., 2009, and references therein), basically concluding that the presence of water causes a strong

absorbance and consequently a decrease in reflectance in the near-infrared spectra of soils.

In general, low signal attenuation can be expected for (peak) winter month atmospheres, especially for clear sky conditions, due to relatively low humidity levels. An effect that still illustrates challenges for the interpretation of IRT images is due to the roughness of the investigated surface (Wu et al., 2009). In most studies the assumption that the scene elements are isothermal, smooth and homogenous is used (Danilina et al., 2006). Consequently supposing that the object of interest is Lambertian, i.e. behaves as a perfect diffuser and emits and reflects radiation isotropically. Mushkin et al. (2007) observed that the effective emissivity spectra of rough surfaces are different from those of perfectly smooth surfaces of the same composition due to multiple scattering among roughness elements. Yet, they only found an up to 3% reduction in the spectral contrast due to sub-pixel surface roughness variations. This might also be the case for situations similar to the presented application as size of the granules, i.e. the sub pixel structures, are much smaller than the pixel size (0.5 to 1 m).

Also whether the surface temperature, and possibly even the composition, of the aerosol mixture of the powder cloud can be measured is an open question. Visualization of air flows on the qualitative level is common practice for various applications (Narayanan et al., 2003; Carlomagno and Cardone, 2010) and, as presented in this study, provides impressive footage of powder snow avalanches. Usually a tracer is injected into the flow field. In our case the tracer is already present by snow particles of the entrained snow which are transported into the powder cloud. Similar concepts as applied for satellite remote sensing of high-level clouds, such as cirrus (Fu et al., 1998), might be transferable to avalanche powder clouds.

A possible further application of IRT could be the differentiation of flow regimes in the deposition area. As shown earlier the warmest part of an avalanche is located in the dense core, e.g. center (red and pink) of avalanche #2 in Fig. 6b, whereas layers with less mass or where less friction occurred are cooler (yellow and orange areas in Fig. 6b). Especially the lookers-left (South) side ~~of the deposition~~ thin-deposit area in Fig.~~6b appears to be~~ 6b might be associated with the deposits of a fluidized layer (Issler et al., 2008) . The IRT observations of this thin-deposit area are in agreement with the field observation criteria for fluidized layers as described by Issler et al. (2008): (1) rapid decrease of deposit thickness, (2) snowballs of various sizes embedded in a matrix of compacted fine-grained snow, (3) large snowballs lying on top of the deposit and (4) fewer snowballs per unit area than on the dense deposit.

~~Deposits~~ For the investigated avalanche the deposits from the powder cloud ~~have~~ had consistently lower temperatures than the warm dense core despite the fact that the powder cloud (at least from one avalanche) traveled as far downhill as the dense core. Two distinct processes may contribute to this fact: (i) A preferential ejection of colder and lighter surface ~~snow layers already initiates suspension~~ with colder snow while the dense core may have a higher fraction of snow from lower layers in the profile and therefore with a higher temperature. (ii) The particle concentration in the suspension layer is low and therefore molecular dissipation of kinetic energy and exchange of sensible and latent heat happens largely between air and snow and not between snow and snow particles as in the dense core. This leads to a rapid adoption of temperatures close to the air temperature for the suspended snow.

Furthermore, the IRT results can be qualitatively interpreted in a similar way as a laser scan to identify areas where deeper or shallower erosion occurred, e.g. see ~~step-down entrainment~~ entrainment by secondary release below the rock face for avalanche #2 (Fig. 6b). For this avalanche we exemplary calculated the release mass solely by using information from the IRT pictures and manually measured snow profiles in the release. Therefore, the IRT picture was georeferenced in a GIS software and shallower and deeper release layers were identified. The (IRT) surface temperature of these layers were combined with the snow height of the corresponding temperature in the conducted snow profile in the release. This resulted in a calculated release mass of 457 t which is similar to the mass measured with the terrestrial laser scan (502 t). This depicts a rough yet quick and efficient method to estimate the release mass of an avalanche. As shown in this study, the release and entrainment depth does not only define the overall mass of snow but equally important its temperature. IRT pictures and videos provide an intuitive and easy ~~to acquire measure to~~ way to identify these relevant erosion processes (Fig. 6).

6 Conclusions

We conducted full-scale avalanche experiments at the Flelapass field site above Davos (Switzerland) to investigate the distribution of snow temperatures in avalanche deposits and identify the sources of thermal energy in dry avalanches. A further goal was to test the usability of infrared radiation thermography (IRT) in this context.

For the investigated similar avalanches the temperature increase due to friction ~~was mainly~~ has been shown to dependent on the elevation the avalanche dropped. The contribution to the total temperature increase by erosion processes was shown to be quite variable, depending on the release depth and snow temperatures of the entrained snow. The warmest temperatures were observed in the center of the avalanche deposits and thus represented the dense core of the flowing avalanche.

The IRT camera allowed to observe the avalanche phenomenon with different eyes and provides a lot of potential for more detailed research in the field of avalanche dynamics, both quantitative and qualitative. It is still necessary to further verify the measurements and define to which extent

absolute snow surface temperatures can be measured. Then, the spatial distribution of surface temperatures can help in the interpolation of profile temperatures measured by hand.

Our results allow for a more comprehensive understanding of snow temperatures in avalanche flow and their consequences on flow regimes. This information can directly be used to verify and enhance the performance of avalanche dynamics models and is thus of great interest for practitioners.

Acknowledgements. Funding for this research has been provided through the Interreg project STRADA and STRADA 2 by the following partners: Amt fr Wald Graubnden, Etat du Valais, ARPA Lombardia, ARPA Piemonte, Valle dAosta, Regione Lombardia. The authors would like to thank all the people who helped gathering the data during the field experiments and Perry Bartelt for his valuable input. Thanks to Vali Meier from the SOS Service Jakobshorn (Davos) and his team for the great support.

References

Armstrong, R. L. and Brun, E.: Snow and Climate: Physical Processes, Surface Energy Exchange and Modeling, Cambridge University Press, Cambridge, UK, 222 pp., 2008.

Bartelt, P., Bühler, Y., Buser, O., Christen, M., and Meier, L.: Modeling mass-dependent flow regime transitions to predict the stopping and depositional behavior of snow avalanches, J. Geophys. Res., 117, http://dx.doi.org/10.1029/2010JF001957, 2012.

Bates, B., Ancey, C., and Busson, J.: Visualization of the internal flow properties and the material exchange interface in an entraining viscous Newtonian gravity current, Environmental Fluid Mechanics, 14, 501–518, 2014.

Brenning, A., Gruber, S., and Hoelzle, M.: Sampling and statistical analyses of BTS measurements, Permafrost and Periglacial Processes, 16, 383–393, 2005.

Carlomagno, G. and Cardone, G.: Infrared thermography for convective heat transfer measurements, Experiments in Fluids, 49, 1187–1218, doi:10.1007/s00348-010-0912-2, http://dx.doi.org/10.1007/s00348-010-0912-2, 2010.

Danilina, I., Mushkin, A., Gillespie, A., O'Neal, M., Pietro, L., and Balick, L.: Roughness effects on sub-pixel radiant temperatures in knetically isothermal surfaces, in: RAQRS II: 2nd International Symposium on Recent Advances in Quantitative Remote Sensing, Torrent (Valencia), Spain, 25-29 September 2006, 2006.

Dozier, J. and Warren, S. G.: Effect of viewing angle on the infrared brightness temperature of snow, Water Resources Research, 18, 1424–1434, doi:10.1029/WR018i005p01424, http://dx.doi.org/10.1029/WR018i005p01424, 1982.

Fierz, C., Armstrong, R., Durand, Y., Etchevers, P., Greene, E., McClung, D., Nishimura, K., Satyawali, P., and Sokratov, S.: The international classification for seasonal snow on the ground, IHP-VII Technical Documents in Hydrology, IACS Contribution N1, UNESCO-IHP, Paris., 83, 2009.

Fu, Q., Yang, P., and Sun, W.: An accurate parameterization of the infrared radiative properties of cirrus clouds for climate models, Journal of climate, 11, 2223–2237, 1998.

Gauer, P., Issler, D., Lied, K., Kristensen, K., and Sandersen, F.: On snow avalanche flow regimes: inferences from observations and measurements, in: Proceedings, International Snow Science Workshop ISSW 2008, Whistler, Canada, pp. 717–723, 2008.

Hori, M., Aoki, T., Tanikawa, T., Hachikubo, A., Sugiura, K., Kuchiki, K., and Niwano, M.: Modeling angular-dependent spectral emissivity of snow and ice in the thermal infrared atmospheric window, Appl. Opt., 52, 7243–7255, doi:10.1364/AO.52.007243, http://ao.osa.org/abstract.cfm?URI=ao-52-30-7243, 2013.

Issler, D., Errera, A., Priano, S., Gubler, H., Teufen, B., and Krummenacher, B.: Inferences on flow mechanisms from snow avalanche deposits, Annals of Glaciology, Vol 49, 2008, 49, 187–192, 2008.

Lewkowicz, A. G. and Ednie, M.: Probability mapping of mountain permafrost using the BTS method, Wolf Creek, Yukon Territory, Canada, Permafrost and Periglacial Processes, 15, 67–80, 2004.

Meola, C. and Carlomagno, G. M.: Recent advances in the use of infrared thermography, Measurement Science and Technology, 15, R27, http://stacks.iop.org/0957-0233/15/i=9/a=R01, 2004.

Mushkin, A., Danilina, I., Gillespie, A. R., Balick, L. K., and McCabe, M. F.: Roughness effects on thermal-infrared emissivities estimated from remotely sensed images, in: Remote Sensing, pp. 67 492V–67 492V, International Society for Optics and Photonics, 2007.

Naaim, M., Durand, Y., Eckert, N., and Chambon, G.: Dense avalanche friction coefficients: influence of physical properties of snow, Journal of Glaciology, 59, 771–782, doi:10.3189/2013JoG12J205, http://www.ingentaconnect.com/content/igsoc/jog/2013/00000059/00000216/art00015, 2013.

Narayanan, V., Page, R., and Seyed-Yagoobi, J.: Visualization of air flow using infrared thermography, Experiments in fluids, 34, 275–284, 2003.

Schirmer, M. and Jamieson, B.: Limitations of using a thermal imager for snow pit temperatures, The Cryosphere, 8, 387–394, doi:10.5194/tc-8-387-2014, http://www.the-cryosphere.net/8/387/2014/, 2014.

Shea, C. and Jamieson, B.: Some fundamentals of handheld snow surface thermography, Cryosphere, 5, 55–66, doi:10.5194/tc-5-55-2011, 2011.

Shea, C., Jamieson, B., and Birkeland, K. W.: Use of a thermal imager for snow pit temperatures, The Cryosphere, 6, 287–299, doi:10.5194/tc-6-287-2012, http://www.the-cryosphere.net/6/287/2012/, 2012.

Snyder, W. C., Wan, Z., Zhang, Y., and Feng, Y.-Z.: Classification-based emissivity for land surface temperature measurement from space, International Journal of Remote Sensing, 19, 2753–2774, doi:10.1080/014311698214497, http://dx.doi.org/10.1080/014311698214497, 1998.

Sovilla, B.: Field experiments and numerical modelling of mass entrainment and deposition processes in snow avalanches., Dissertation no. 15462, Swiss Federal Institute of Technology, Zürich, 2004.

Sovilla, B., Burlando, P., and Bartelt, P.: Field experiments and numerical modeling of mass entrainment in snow avalanches, Journal of Geophysical Research-earth Surface, 111, doi:10.1029/2005JF000391, 2006.

Sovilla, B., Margreth, S., and Bartelt, P.: On snow entrainment in avalanche dynamics calculations, Cold Regions Science and Technology, 47, 69–79, doi:10.1016/j.coldregions.2006.08.012, 2007.

Steinkogler, W., Gaume, J., Löwe, H., Sovilla, B., and Lehning, M.: Granulation of snow: from tumbler experiments to discrete element simulations, Journal of Geophysical Research - Earth Surface , submitted, 2014a.

Steinkogler, W., Sovilla, B., and Lehning, M.: Influence of snow cover properties on avalanche dynamics, Cold Regions Science and Technology, 97, 121–131, doi:10.1016/j.coldregions.2013.10.002, http://www.sciencedirect.com/science/article/pii/S0165232X13001535, 2014b.

Valero, C. V., Jones, K. W., Bühler, Y., and Bartelt, P.: Release temperature, snow-cover entrainment and the thermal flow regime of snow avalanches, Journal of Glaciology, 61, 173, 2015.

Vera, C., Feistl, T., Steinkogler, W., Buser, O., and Bartelt, P.: Thermal Temperature in Avalanche Flow, Proceedings, International Snow Science Workshop ISSW 2012, Anchorage, Alaska, pp. 32–37, 2012.

Wu, C.-Y., Jacobson, A. R., Laba, M., and Baveye, P. C.: Accounting for surface roughness effects in the near-infrared reflectance sensing of soils, Geoderma, 152, 171 – 180, doi:http://dx.doi.org/10.1016/j.geoderma.2009.06.002, http://www.sciencedirect.com/science/article/pii/S0016706109001803, 2009.